Monitoring Circumferential Welds in Canisters with Helical Ultrasonic Guided Waves

P. SHIVASHANKAR, NATHAN WILSON, GUAN-WEI LEE and SALVATORE SALAMONE

ABSTRACT

Welded regions in canisters that are used to store industrial chemicals, fuels, gases, spent nuclear fuels, etc., are susceptible to damage due to stress corrosion cracking and fatigue failure. Hence, monitoring their integrity over time is essential to prevent leaks. One way to monitor the canister welds' integrity is through active SHM with helical-guided ultrasonic waves (HGUW). When HGUW interact with defects in welds, their signature is altered, and based on this, the regions of defects can be located and mapped. This work demonstrates the mapping of damaged regions in circumferential welds in canisters using HGUW. A canister cut section, made by circumferentially welding two rings, was used as the test structure to demonstrate the mapping methodology. Two circumferential PZT arrays, each one on the opposing side of the weld, provided a network of paths that enabled monitoring of the weld all around the circumference. The presence or absence of damage in any section of the weld can be determined by analyzing the wave propagating along a path passing through the specific region. By combining information from all such paths, a map indicating the location of damages was constructed. Accordingly, waveforms from all paths of the network were acquired, and the information from them was used to generate a map via the Reconstruction Algorithm for Probabilistic Inspection of Damage (RAPID) method to locate the damaged area. The successful mapping of the damaged region established this technique as a valid option for the long-term monitoring of circumferential welds.

INTRODUCTION

In thin hollow cylinders, excitation by an omnidirectional actuator such as a PZT disc causes the propagation of helical-guided ultrasonic waves (HGUW). These are Lamb-type guided waves that travel in a spiral fashion about the cylinder. As such, between an actuator and a sensor, these waves can travel along multiple paths, called the orders, and arrive at different durations. Researchers have recently developed techniques to localize and characterize various types of damage in thin metallic pipes using HGUW [1–5]. For

P. Shivashankar, N. Wilson, G.-W. Lee, & S. Salamone, Smart Structures Research Laboratory (SSRL), Maseeh Department of Civil, Architectural and Environmental Engineering, The University of Texas at Austin, Austin, TX 78712, USA

instance, Dehghan-Niri and Salamone used the first nine orders of the HGUW to map three regions on a thin steel pipe where there was a 40% loss in wall thickness. Subsequently, Livadiotis et al. [3] used the first five orders of HGUW to not only locate the regions of thickness loss but also qunatify thickness loss. In a new attempt, Shivashankar et al. [4, 5] used the scattered HGUW signals to propose a method to identify the length of crack-like defects in hollow cylinders.

These studies showcase the effectiveness of using the HGUW for locating and characterizing various types of damage in hollow cylindrical structures. Two factors that make the HGUW-based mapping particularly enticing are the requirement of a minimal number of transducers and the ease of experimentation. In terms of transducers to generate and receive HGUW, only a few low-profile PZT discs need to be bonded to the cylinder's outer surface for implementation. With two circumferential arrays of sparsely distributed PZT discs, the entire region enclosed between the arrays can be effectively mapped. In the matter of ease of experimentation, the test only requires PZTs to be actuated one at a time while the sensors acquire the responses. For these reasons, this work also uses HGUW as the basis for locating damages in circumferential welds in canisters.

In hollow cylindrical structures, such as canisters, a region that is more susceptible to damage is the part containing welds, particularly the circumferential welds. Circumferential welds are a prominent feature of canisters, regardless of their size. Large canisters that store spent nuclear fuels are manufactured by stacking and welding multiple cylindrical sections circumferentially. Even in smaller ones, where a single sheet of metal is rolled into a cylinder, the top and bottom ends are capped and welded circumferentially.

Welded regions are susceptible to damage due to stress corrosion cracking and fatigue failure. Hence, monitoring them to identify the onset and propagation of damage is essential to safeguard the structure's integrity and avoid leaks. To this end, this work demonstrates the mapping of damage in a circumferential weld in a 5.6-inch tall canister cut section using HGUW. Accordingly, the experimental setup is described in the next section, followed by the description of the imaging algorithm and results in the penultimate section. The final section concludes the paper by summarizing and discussing the work and offering remarks on future research.

EXPERIMENT

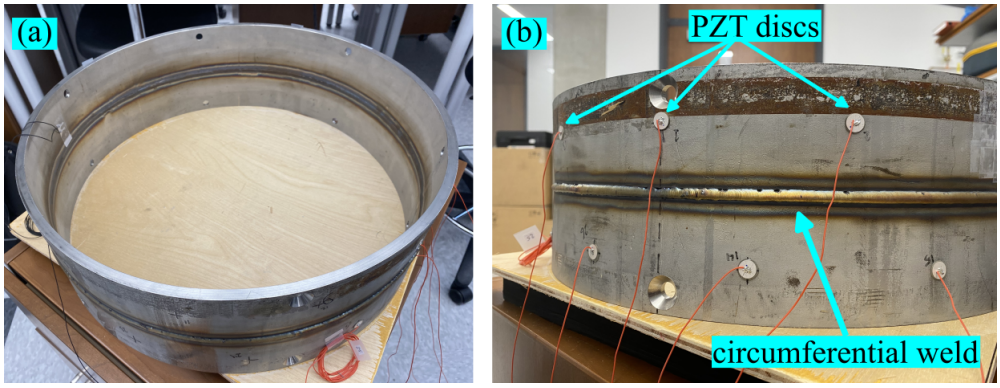

Figure 1. The canister cut specimen with the circumferential weld.

Figure 1 shows the cut section of the canister used in the experiment. The test specimen was 14.2 cm tall, with an approximate outer diameter of 18 inches and a wall thickness of 0.88 cm. The circumferential weld in the structure was the targeted area for investigation. This area is prominent because the weld bead is not ground flush. The weld state shown in this figure was considered to be in the pristine state, and hence, the signals collected from this state were used as the baseline data.

To actuate and receive the HGUW, PZT discs were distributed around the circumference along two arrays, as shown in Figure 1b. Each circumferential array had thirteen identical PZT discs evenly distributed around the circumference. The PZT discs were procured from APC International Ltd. and were of Type 851, with a diameter of 10 mm and a thickness of 0.7 mm. They were bonded to the structure with the two-part Araldite epoxy. The transducers in the top array (numbered 1-13) were used as sensors, while those in the bottom array (numbered 14-26) were used as actuators.

In the experiments, only the first HGUW arrivals were used for mapping. Figure 2 plots all the paths formed by all possible combinations of sensors and actuators. A dense network of paths is still obtained despite using only the first-order arrivals due to the relatively higher number of transducers.

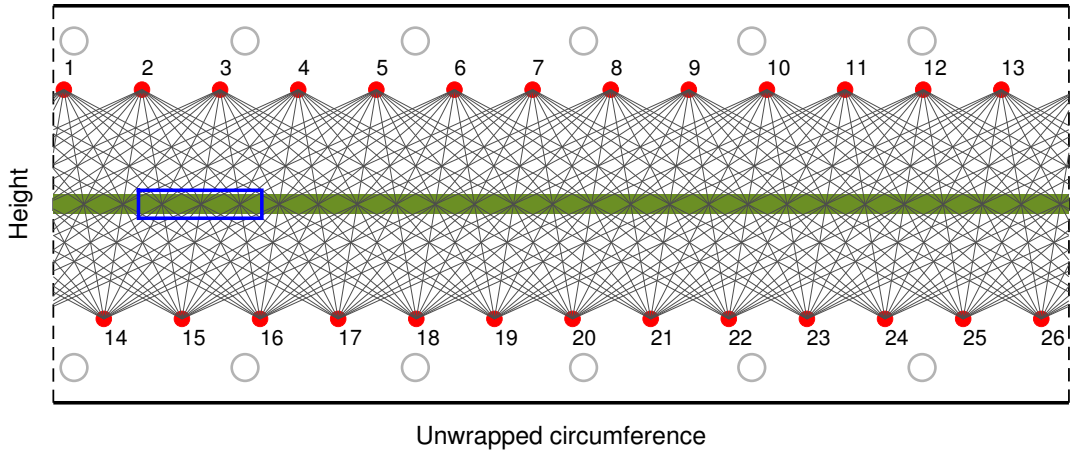

Figure 2. A schematic diagram of the unwrapped canister showing the network of paths, wherein ● indicates the PZT discs, ○ denotes the through holes in the structure, ▬ depicts the circumferential weld, and ▭ outlines the damaged region in the cirumferential weld.

For the purposes of testing the HGUW-based method, artificial damage was introduced in the weld region by grinding down the weld bead over a small circumferential length. Specifically, beginning just below transducer No.2, a 17.6 cm segment of the weld was ground flush using a Dremel tool to emulate a damage scenario. While this does not exactly imitate real-world weld degradation, it is intended primarily to test the method's ability to map regions of weld erosion or material (i.e., thickness) loss. Figures 3a and b show the structure before and after the grinding, respectively.

The excitation signal was a 5-cycle tone burst with a center frequency of 250 kHz. The signal was generated by an Agilent 33522A waveform generator and amplified by a Ritec RPR4000 Pulser Receiver, which was set in the external mode. The generated wave signals were acquired with an NI PXIe-5105 oscilloscope housed in an NI PXIe-

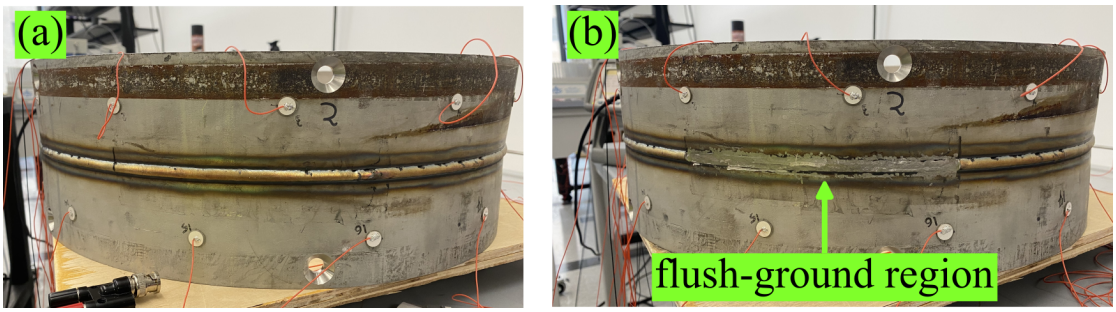

Figure 3. The specimen with (a) pristine and (b) damaged circumferential weld.

1071 chassis. At 250kHz, three Lamb modes, namely the S_0, A_0, and A_1 can exist. The respective wavelengths and group velocities of these three modes are estimated as $\lambda_{S_0} = 1.88$ cm, $\lambda_{A_0} = 1.11$ cm, and $\lambda_{A_1} = 3.29$ cm, and $V_g^{(S_0)} = 2606$ m/s, $V_g^{(A_0)} = 3205.6$ m/s, and $V_g^{(A_1)} = 3509.4$ m/s. Figure 4 shows the pristine and damaged signals for actuation from actuator-17 and responses from sensors 1 and 18. Wave packets are present in all three mode windows, indicating the generation and propagation of all three modes (S_0, A_0, & A_1). However, due to short travel distances, there is a significant overlap of the A_0 and A_1 modes. The shorter height of the specimen may also lead to reflected signals interfering with the first arrivals. Despite these issues, the signals still reflect the changes due to the presence of the "damage". For instance, the path A17-S1 goes through the damaged region, and consequently, a change in the signal signature can be witnessed in the A_0 window. On the other hand, path A17-S8 does not pass through the damaged region, and as expected, the signal along this path does not appear to have been altered significantly. As such, the amplitude-scaled damage indexes estimated from the A_0 window for the respective paths are: $\mathcal{D}_{A17-S1} = 0.01372$ and $\mathcal{D}_{A17-S8} = 0.00503$. The damage indexes are evaluated from the following expression,

$$\mathcal{D} = \max_{t\in[t_1,t_2]} |s_p(t)| \left(\frac{\int_{t_1}^{t_2} [s_d(t) - s_p(t)]^2 \, dt}{\int_{t_1}^{t_2} [s_p(t)]^2 \, dt} \right) \tag{1}$$

where, s_p and s_d indicate the pristine and damaged signals, respectively, and t_1 and t_2, the start and end times of the A_0 window.

Damage indexes were estimated along all the paths, and a map indicating the location of the damage was built. The algorithm used to construct the map is discussed in the following section.

DAMAGE MAPPING BY RAPID

RAPID

A contour map showing the damages in the structure was produced by the RAPID (Reconstruction Algorithm for Probabilistic Inspection of Damage) by aggregating damage information from each individual path. That is, the constructed map is made by summing together the defect distributions of all transducer pairs. The defect distribution for

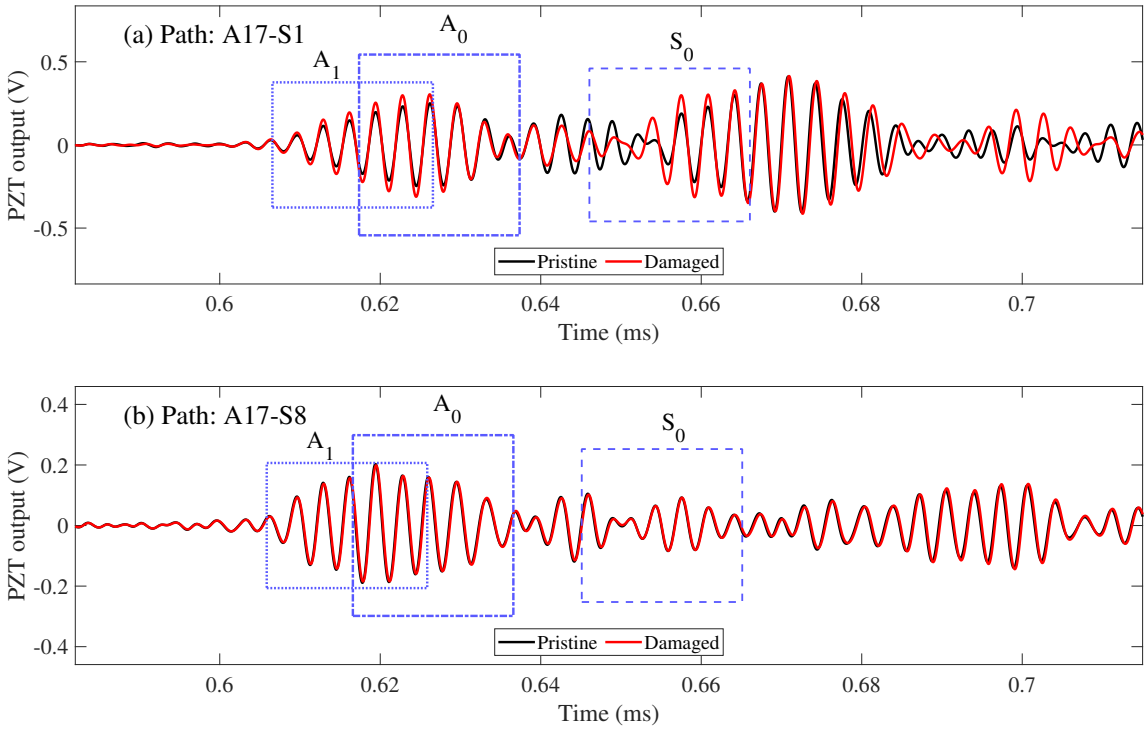

Figure 4. Pristine and damaged wave responses propagating along the paths connecting (a) Actuator-17 and Sensor-1, and (b) Actuator-17 and Sensor-8.

the k^{th} transducer pair is estimated according to,

$$p_k(x,y) = \mathcal{D}_k\left(\frac{-R_k(x,y)}{\beta-1} + \frac{\beta}{\beta-1}\right) \tag{2}$$

where

$$R_k(x,y) = \frac{\sqrt{\left(x-x_k^{(A)}\right)^2 + \left(y-y_k^{(A)}\right)^2} + \sqrt{\left(x-x_k^{(S)}\right)^2 + \left(y-y_k^{(S)}\right)^2}}{\sqrt{\left(x_k^{(S)}-x_k^{(A)}\right)^2 + \left(y_k^{(S)}-y_k^{(A)}\right)^2}} \tag{3}$$

(x,y) denote the coordinates of any point on map, and $\left(x_k^{(A)}, y_k^{(A)}\right)$ and $\left(x_k^{(S)}, y_k^{(S)}\right)$ indicate the coordinates of the k^{th} transducer pair's actuator and sensor locations, respectively. β in Equation 2 is a scaling parameter.

Equation 2 generates a heat map with a set of concentric ellipses with the k^{th} transducer-pair coordinates at the foci. This heat map represents the spatial distribution of damage in the sub-area surrounding the k^{th} transducer pair. As such, the direct path connecting the transducers is specified to have the highest probability of containing the damage. Beyond this direct path, this probability progressively diminishes with each successive elliptical contour. The final heat map–which indicates the presence of the damage–is a sum of the spatial damage distributions of all transducer pairs. As such, the contour map

of the structure is generated from the following equation.

$$P(x,y) = \sum_{k=1}^{k=N} p_k(x,y) \tag{4}$$

TOMOGRAPHIC IMAGE

Figure 5 shows the heat map generated through RAPID with damage indexes obtained from 169 transducer pairs. A region of higher intensity implies the presence of damage in that region. Cross-referencing this heat map with Figure 2 shows that the high-intensity region is in the same locality as the damage. Though the heat map correctly indicates the damaged region on the canister-ring specimen, the identified region is broad in nature and does not convey anything quantitatively. To identify the exact location of the damage, a threshold was set, and the regions with intensities higher than the threshold were designated to contain the damage. For this study, the threshold was chosen to be 0.85. Regions with intensities above 0.85 were demarcated and marked as potential regions containing the damage.

The first image in Figure 6 shows the heat map with the contours marking the high-intensity regions. The second image superimposes these regions on the schematic diagram, wherein it can be seen that the regions identified from the experiments closely match the actual damaged area in the weld.

Figure 5. The tomographic image obtained from RAPID.

The successful detection of the damaged region in the circumferential weld validates the HGUW-based tomographic mapping as a reliable method for monitoring circumferential welds. Future studies will explore the mapping of various types of weld defects to establish the presented approach as a viable option. Additionally, the incorporation of higher-order arrivals will be investigated to enhance the localization of damages.

Another important direction for future work involves examining how real-world factors influence tomographic mapping. In practical applications, factors such as operating temperature, transducer sensitivity decline over time, and the long-term integrity of bonding layers can significantly impact the generated and acquired HGUW signals. Therefore, it is crucial to evaluate and measure their effects. Future research will review relevant literature [6, 7] and conduct experimental studies on each factor to determine

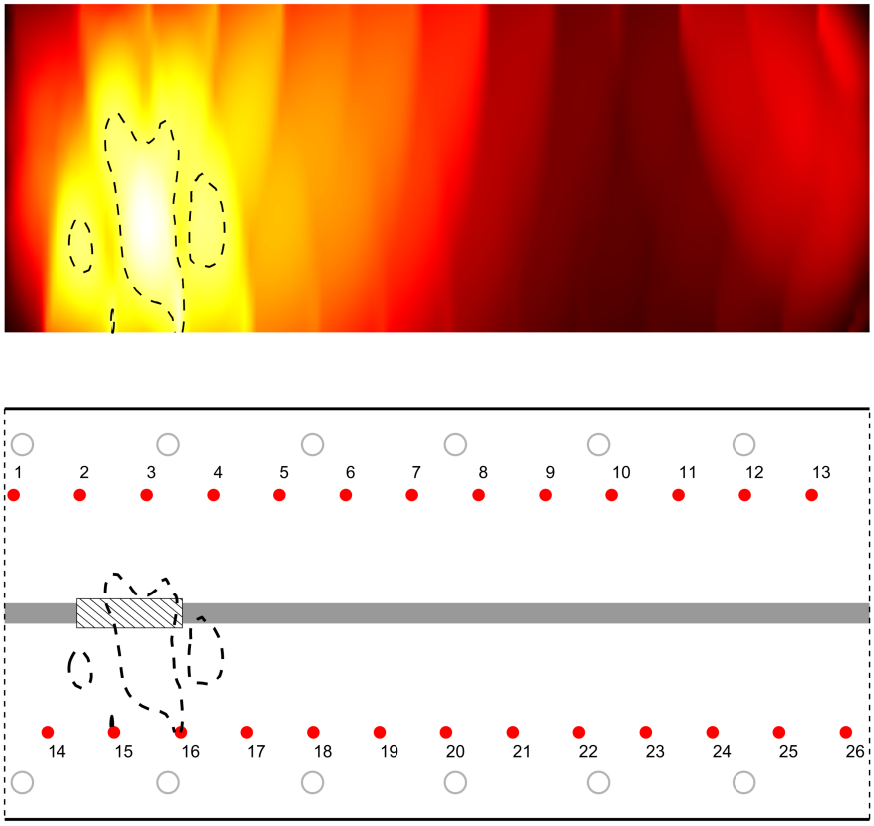

Figure 6. Marking the regions of high intensity and superimposing these areas on the schematic diagram illustrating the damage.

their influence on the signals and the uncertainties they cause. Based on these results, suitable correction or compensation methods will be developed to reduce their effects and improve the method's robustness in field conditions.

CONCLUSION

This work investigated the possibility of using helical-guided ultrasonic waves (HGUW) to monitor the circumferential welds in canisters. Earlier studies have demonstrated the effectiveness of HGUW-based mapping in locating corrosive defects (such as wall thinning) in hollow cylindrical structures. Establishing the capability of this method to map damages in welds would extend this technology for holistic monitoring of canisters. Accordingly, the method's ability to map damages in circumferential welds was tested on a canister cut specimen. Damage was created by grinding a small section of the weld bead to simulate weld erosion or material loss. PZT discs were bonded to the structure ins two circumferential arrays to create a dense network of paths that pass through the circumferential weld. The damage was successfully mapped with the A_0-like mode of the HGUW using the RAPID method. This successful demonstration showcases the

method's applicability for long-term monitoring of circumferential welds in canisters. With this successful validation as a starting point, future studies will investigate mapping more subtle damages and extend the method for practical applications.

ACKNOWLEDGMENT

The authors thank the Idaho National Laboratory for its support of this work (Contract No. #303940).

REFERENCES

1. Dehghan-Niri, E. and S. Salamone. 2015. "A multi-helical ultrasonic imaging approach for the structural health monitoring of cylindrical structures," *Structural health monitoring*, 14(1):73–85.
2. Livadiotis, S., A. Ebrahimkhanlou, and S. Salamone. 2021. "Monitoring internal corrosion in steel pipelines: a two-step helical guided wave approach for localization and quantification," *Structural health monitoring*, 20(5):2694–2707.
3. Livadiotis, S., K. Sitaropoulos, A. Ebrahimkhanlou, and S. Salamone. 2023. "Acoustic emission monitoring of corrosion in steel pipes using Lamb-type helical waves," *Structural health monitoring*, 22(2):1225–1236.
4. Shivashankar, P., J. Sohn, S. Livadiotis, and S. Salamone. 2024. "Notch characterization in pipes from the scattering of helical-guided ultrasonic waves," in *Health Monitoring of Structural and Biological Systems XVIII*, SPIE, vol. 12951, pp. 470–484.
5. Shivashankar, P., J. Sohn, and S. Salamone. 2025. "Tracking growth of crack-like defects in hollow cylindrical structures from the stepped-wavelength scattering of helical guided ultrasonic waves," *Mechanical Systems and Signal Processing*, 236:112918.
6. Raghavan, A. and C. E. Cesnik. 2008. "Effects of elevated temperature on guided-wave structural health monitoring," *Journal of Intelligent Material Systems and Structures*, 19(12):1383–1398.
7. Yang, K., Z. Yang, H. Yang, J. Zhou, Z. R. Zhang, L. Wang, Z. Tian, S. Kim, and J. B. Harley. 2025. "Dataset on guided waves from long-term structural health monitoring under uncontrolled and dynamic conditions," *Scientific Data*, 12(1):1–19.